These results demonstrate that redox chemical diffusion experiments do not a priori allow characterization of the diffusion coefficient of an oxygen species in a Fe-bearing aluminosilicate melt. Differences in values of diffusion coefficients extracted from a redox experiment and an oxygen tracer diffusion experiment on the same melt composition would therefore reflect that the two procedures are measuring different things. Our experiments additionally demonstrate that the cation-diffusion response to a redox driving force allows for relatively rapid chemical segregation in a melt; the mechanism should perhaps be considered as contributing to the concentric segregation microstructures frequently described for primitive chondrules (23).

REFERENCES AND NOTES

1. P. C. Hess, *Origins of Igneous Rocks* (Harvard Univ. Press, Cambridge, MA, 1989), chap. 5.
2. P. L. Roeder and E. F. Osborn, *Am. J. Sci.* **264**, 428 (1966).
3. T. Dunn, *Geochim. Cosmochim. Acta* **46**, 2293 (1982).
4. D. Canil and K. Muehlenbachs, *ibid.* **54**, 2947 (1990).
5. T. Dunn, *ibid.* **47**, 1923 (1983).
6. H. D. Schreiber, S. J. Kozak, A. L. Fritchman, D. S. Goldman, H. A. Schaeffer, *Phys. Chem. Glasses* **27**, 152 (1986).
7. R. F. Wendlandt, *Contrib. Mineral. Petrol.* **108**, 463 (1991).
8. G. B. Cook, R. F. Cooper, T. Wu, *J. Non-Crys. Solids* **120**, 207 (1990).
9. J. Zarzycki, *Glasses and the Vitreous State* (Cambridge Univ. Press, Cambridge, UK, 1991), chap. 11.
10. H. Schmalzried, *Solid State Reactions* (Verlag Chemie, Weinheim, Federal Republic of Germany, ed. 2, 1981), chap. 8.
11. T. Wu and D. L. Kohlstedt, *J. Am. Ceram. Soc.* **71**, 540 (1988); D. L. Kohlstedt, C. Goetze, W. B. Durham, J. VanderSande, *Science* **191**, 1045 (1976).
12. E. B. Watson, *Earth Planet. Sci. Lett.* **52**, 291 (1981).
13. H. Schmalzried, *Ber. Bunsenges. Phys. Chem.* **87**, 551 (1983).
14. T. L. Grove, *Contrib. Mineral. Petrol.* **78**, 298 (1981); D. L. Kohlstedt and S. J. Mackwell, *ibid.* **95**, 226 (1987).
15. J. K. R. Weber *et al.*, *Rev. Sci. Instrum.* **65**, 456 (1994). Basalt droplet levitation required a gas flow rate of ~3 l min^{-1} (jet velocity of ~18 m s^{-1}). Heating a droplet to 1400°C, by focusing the laser, took 5 to 7 s; quenching occurred more rapidly. At the 1400°C processing temperature, the actual temperature across the droplet varied by ~50°C; the bottom of the droplet was cooler than the sides.
16. The composition (oxide weight percent) of the starting material is SiO_2, 43.7; TiO_2, 2.7; Al_2O_3, 14.3; FeO,12.2; MnO, 0.2; MgO, 9.5; CaO, 11.4; Na_2O, 3.3; K_2O, 1.1; P_2O_5, 0.7 (*19*). The glass was prepared by melting ~10 g of finely powdered rock in a high-purity Al_2O_3 crucible at 1450°C for 30 min at $p_{O_2} = 10^{-8}$. The melt was quenched within the controlled environment. Any glass contaminated with excess alumina, as determined by electron-probe spectroscopy, was ground away. The resultant glass, black in color, was chemically homogeneous and displayed no crystallization to the resolution of conventional optical microscopy.
17. J. Myers and H. P. Eugster, *Contrib. Mineral. Petrol.* **82**, 75 (1983).
18. 2.5 MeV α-particles ($^4He^{2+}$) were employed. Backscattering spectra were analyzed by an iterative simulation process [L. R. Doolittle, *Nucl. Instrum. Methods Phys. Res.* **B9**, 344 (1985)], which is based on the well-established database of ion-stopping and ion-backscattering cross sections [for example, J. F. Ziegler, J. P. Biersack, U. Littmark, *The Stopping and Range of Ions in Solids* (Pergamon, New York, 1985)]. The α-particle beam has a spot diameter of ~1 mm; the flattened bottoms of quenched droplets could be easily and directly analyzed. The beam spans an arc of ~12° on the tops of droplets; this produces an error in backscattering yield of ~10%, for which a correction is accomplished in the simulation analysis.
19. R. F. Cooper, J. B. Fanselow, D. B. Poker, *Geochim. Cosmochim. Acta* **60**, 3253 (1996).
20. A. Muan and E. F. Osborn, *Phase Equilibria Among Oxides in Steelmaking* (Addison-Wesley, Reading, MA, 1965).
21. C. Wagner, *J. Colloid Sci.* **5**, 85 (1950); D. L. Ricoult and H. Schmalzried, *Ber. Bunsenges. Phys. Chem.* **90**, 135 (1986).
22. The gradient in oxygen chemical potential in the residual oxidized melt is physically manifest by a gradient in the concentration of polarons (electron holes), which are distorted Fe^{3+} modifier–O^{2-} bonds; it is through these distortions, these "point defects," that modifier divalent cation diffusion occurs (*19*).
23. Some reduced, primitive chondrules, for example, in Semarkona (LL3), display concentric rings of internal metal precipitation [for example, J. T. Wasson, *Meteorites: Their Record of Early Solar System History* (Freeman, New York, 1985), chap. 7]. Such a microstructure is characteristic of a dynamic reduction process for the liquid that is a mirror-image of oxidation, that is, oxygen is ablated at the surface, divalent cations diffuse inward while electron holes counter-diffuse toward the surface; iron precipitates at an internal reduction front [compare with, H. Schmalzried, *Ber. Bunsenges. Phys. Chem.* **88**, 1186 (1984)]. We have evidenced this reduction process in recent experiments on a synthetic basalt analog.

24. This work was funded, in part, by a grant (to R.F.C.) from the National Aeronautics and Space Administration, Division of Microgravity Sciences and Applications (NAGW-2835). Rutherford backscattering spectroscopy was performed at the Center for Surface Modification and Characterization at Oak Ridge National Laboratory, which is sponsored by the Division of Materials Sciences, U.S. Department of Energy (DE-AC05-96OR22464).

29 April 1996; accepted 7 October 1996

The Edge of Time: Dating Young Volcanic Ash Layers with the ^{40}Ar-^{39}Ar Laser Probe

Yanshao Chen, Patrick E. Smith, Norman M. Evensen, Derek York, Kenneth R. Lajoie

Argon-40–argon-39 single-crystal dating of young (5000 to 30,000 years ago) volcanic ash layers erupted from the Mono Craters, California, shows that the method can yield meaningful ages in Holocene tephra. Because of ubiquitous xenocrystic contamination, the data do not form isochrons but plot in wedge-shaped regions on an argon isotopic diagram. The upper boundary of the region is an isochron matching the ^{14}C-derived age of the eruption. Such contamination-related patterns may be common in dating young materials by the single-crystal method. Argon dating by this method can help refine the time scale of physical and biological evolution over the past 100,000 years.

Nature has endowed the potassium-argon geochronometer with great power. The 1.3-billion-year half-life of the parent, ^{40}K, allows the geochronometer to be used to date events back to the creation of the solar system, while the efficiency with which minerals typically exclude ambient argon at their formation makes it a sensitive tool for dating the recent past. The ^{40}Ar-^{39}Ar method of reading the K-Ar clock and the laser step-heating procedure for the analysis of single grains add to its versatility and resolution (*1*). Argon dating of the last 100,000 years, while technically difficult, can complement ^{14}C and other dating tools, and could be invaluable in resolving uncertainties and ambiguities in other methods.

Dating of sanidine crystals separated from rhyolitic lavas from the Mono Craters, California, demonstrated the feasibility of using ^{40}Ar-^{39}Ar single-crystal laser-probe analysis to date suitable material as young as 12.5 thousand years ago (ka) with approximately 5% precision (3). However that study did not rule out the possible presence of excess radiogenic ^{40}Ar (4) at a uniform concentration in the sanidine crystals, corresponding to a quantum of erroneous excess age, because no independent measurement of the eruptive age was available. We have therefore analyzed sanidine crystals from three tephra layers, also in the Mono Craters area, for which ^{14}C age control exists.

The Mono Craters, a string of volcanic domes, flows, and explosion craters in central California, erupted episodically in the late Quaternary, depositing layers of ash in adjacent Mono Lake and in nearby meadows. We analyzed two ash layers (WCA-8 and WCA-15) in the late Pleistocene Wilson Creek Formation (WCF), a lacustrine silt deposited during the last deep-water phase of Mono Lake (5). We also dated an ash layer (CMA-13) in a sequence of Holocene peat deposits in Crooked Meadow, directly southeast of Mono basin (6). Inter-

Y. Chen, P. E. Smith, N. M. Evensen, D. York, Department of Physics, University of Toronto, 60 Saint George Street, Toronto, Ontario M5S 1A7, Canada.
K. R. Lajoie, U.S. Geological Survey, 345 Middlefield Road, MS-977, Menlo Park, CA 94025–3591 USA.

polation between ^{14}C-dated horizons in the sections, together with correction from ^{14}C years to calendar years, yields estimates of 4.6 ± 0.1, 25.0 ± 1.0 and 30.8 ± 0.9 ka for samples CMA-13, WCA-15 and WCA-8, respectively (*7*).

Analyses of 42 sanidine crystals from ash layer WCA-15 (*8*), instead of lying along an isochron line on the argon isotope correlation diagram (*9*), define a wedge-shaped area (Fig. 1), with only one sample plotting outside it. In Fig. 1, both the upper, younger boundary and the lower, older boundary of the wedge are isochrons constrained to pass through the modern atmospheric value ($^{36}Ar/^{40}Ar$ = 1/295.5) and having slopes determined from the data points (*10*). Such a wedge is therefore a wedge of time, which we term a "sphenochron" (from the Greek word σφην, a wedge). The upper edge of this time wedge, characterizing the youngest material found in the sample, represents the time of eruption, and agrees well with the age of the sample inferred from the calibrated ^{14}C data. Most of the crystals, which plot significantly below the upper boundary of the wedge, must either be older than the eruption of the ash, or must appear older as a result of excess ^{40}Ar incorporated at their formation.

Although excess argon is potentially a serious problem in dating igneous materials (*12*), sanidine has long been considered essentially free from excess (*2*). In these young samples, however, even a small excess would significantly affect the apparent age. A rhyolitic magma chamber, such as that which produced the Mono Craters, is likely to be a reservoir of excess ^{40}Ar, both that derived from crustal rocks incorporated into the magma, and that produced in situ during the lifetime of the magma chamber (*13*). However, the varying incorporation of excess argon into sanidine phenocrysts should result in dispersion along an isochron with the correct age and an initial $^{40}Ar/^{36}Ar$ ratio higher than that of atmosphere. The sphenochron represents nearly the opposite situation: a dispersion in ages with no evidence for a nonatmospheric initial ratio.

We therefore regard the other possibility, that many of the sanidine crystals are older than the eruption event, as more likely. Such older crystals could result from closure of the argon system in phenocrysts formed before eruption or from the incorporation of xenocrysts from earlier eruptive events. Diffusion calculations suggest that sanidine phenocrysts in a silicic magma chamber should retain argon for at most days or weeks, and certainly not for thousands of years (*15*). We therefore favor a xenocrystic origin of the sanidine crystals that plot significantly below the upper boundary of the sphenochron. Xenocrysts defining the lower boundary of the sphenochron may provide a minimum age for the earliest eruption from the corresponding vent.

Evidence supporting this interpretation is shown by replotting single-crystal ^{40}Ar-^{39}Ar data for anorthoclase crystals from the Hüttenberg tephra layer of the East Eifel Volcanic Field of Germany (*16*). There the actual eruption age of 215 ka was determined from crystals in the most mafic lapilli, which yielded a well-defined isochron. Crystals from more differentiated samples, when rescaled (Fig. 1), form a wedge-shaped area similar to the one seen in the Mono Craters tephra data; the 215-ka eruption age isochron forms the upper boundary of this wedge.

Twenty-eight sanidine crystals from ash layer WCA-8 and 23 from CMA-13 display a similar pattern, although the fewer samples provide a sparser image of the sphenochrons (Fig. 2). As above, the upper boundaries of the sphenochrons agree to 2σ with the ages inferred from the calibrated ^{14}C data. The lower boundary of the WCA-8 sphenochron (with the exception of the 710 ka outlier noted above) is similar to that of WCA-15 and significantly older than the bottom of the sphenochron for CMA-13.

Ash layers WCA-8 and WCA-15 each contain one sanidine crystal with a significantly greater age than the remainder. Their apparent ages of 710 and 498 ka

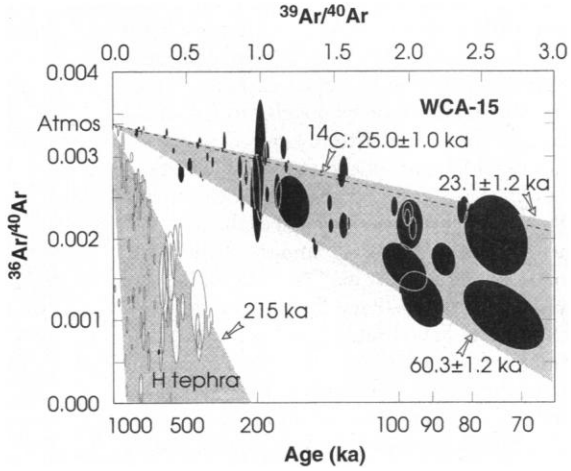

Fig. 1. $^{36}Ar/^{40}Ar$ versus $^{39}Ar/^{40}Ar$ correlation diagram for sanidine crystals from ash layer WCA-15 (filled ellipses), and for comparison, earlier analytical results (*16*) from the differentiated Hüttenberg tephra (H tephra) of the East Eifel volcanic field, Germany (open ellipses). All ellipses show 1σ analytical errors. Shaded areas are "sphenochrons," bounded by isochrons passing through the $^{36}Ar/^{40}Ar$ ratio of modern atmosphere (=1/295.5). The bounding isochrons for WCA-15 are determined by statistical analysis of the argon data (*10*), with the inferred, corrected ^{14}C age of the tephra (*7*) shown as a dashed line for comparison. The upper bound for the H tephra is defined by a 215-ka isochron obtained from anorthoclase crystals from the most mafic lapilli (*16*). See text for further discussion. Note that one small filled ellipse from the WCA-15 ash is within the H tephra region. All data have been normalized to a *J* value of 1.076 × 10^{-4}, and the corresponding age scale plotted at the bottom. The integrated age for all WCA-15 data is 38.8 ± 1.1 ka, and is equivalent to the age that would be obtained from a bulk analysis of all the analyzed crystals.

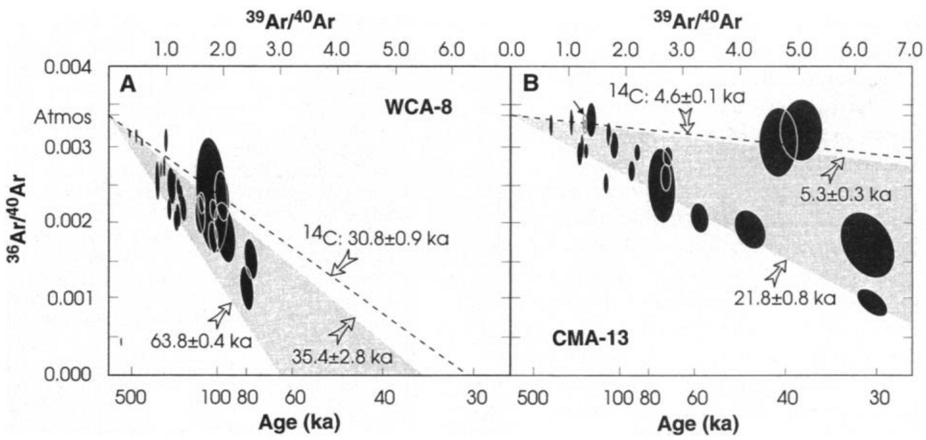

Fig. 2. $^{36}Ar/^{40}Ar$ versus $^{39}Ar/^{40}Ar$ correlation diagrams for sanidine crystals from ash layers WCA-8 (**A**), and CMA-13 (**B**). The ellipses show 1σ analytical errors, except the two concentric open ellipses indicated by the small arrow in (B), which for clarity show 2σ errors. Shaded areas are sphenochrons, bounded by isochrons determined from the argon data, but constrained to pass through the $^{36}Ar/^{40}Ar$ ratio of modern atmosphere (=1/295.5) (*10*). For both samples the inferred, corrected ^{14}C ages of the corresponding tephras (*7*) are shown as dashed lines for comparison. All data have been normalized to a *J* value of 1.076 × 10^{-4}, and the corresponding age scale is plotted at the bottom. The integrated age for WCA-8 data is 44.0 ± 1.2 ka and for CMA-13 is 13.6 ± 0.9 ka.

suggest that they are partially reset sanidine crystals from the 760 ka Bishop Tuff (*14*), which immediately underlies the Mono Craters. There is no way to distinguish a priori whether a particular crystal was partially reset (without step-heating, which is difficult in these young samples).

Sphenochrons provide information on the time of eruption of the particular ash layer analyzed (the upper bounding isochron). If the sphenochron contains only eruptive xenocrysts, the lower bounding isochron puts a lower limit on the age of volcanism near the vent from which the ash was erupted; this may characterize individual vents. Thus tephra layers WCA-8 and WCA-15 may have erupted from the same vent or from closely related vents that opened by about 62 ka, and tephra layer CMA-13 may have erupted from a different vent that opened by about 22 ka.

The existence of sphenochrons has implications for the geochronology of young ash layers, which are widely used as time markers in climatologic, geologic and biologic studies. If, as we propose, the true age of the ash layer is given by the upper boundary of the sphenochron, bulk K-Ar or ^{40}Ar-^{39}Ar dating will yield an integrated age for the eruption (see captions to Figs. 1 and 2) that is too old. The resulting error would be indistinguishable from the effects of excess argon. The magnitude of such an error would depend on the distribution of ages within the sphenochron. Furthermore, even single-crystal dating with insufficient statistics may be misleading. For instance, repeated random selections of five crystals from our data set for WCA-15 yielded apparently good isochrons [as measured by the MSWD (*11*)], but with an incorrect age about half the time. Similar errors arising from xenocrystic contamination can also exist in other isotopic dating systems, depending on the degree to which the xenocrysts are reset in those systems (*17*).

Our previous dating of sanidine phenocrysts from the Mono Craters (*3*) yielded well-defined isochrons, and showed no sign of a sphenochron. Those crystals were taken from a rhyolitic flow rather than an ash layer. Xenocrysts are more likely to be reset in slowly cooling lavas than in rapidly cooling ashfalls. It is also possible that explosive eruptions are more prone to xenocrystic contamination than effusive eruptions.

Our results imply that eruption ages for highly contaminated young tephras ($\leq$30 ka) can be determined by locating the upper boundaries of the associated sphenochrons produced by single-crystal laser analysis (*10*). In appropriate circumstances the ^{40}Ar-^{39}Ar laser probe can be used to date accurately materials from the Holocene to the Archean, from one edge of geologic time to the other.

REFERENCES AND NOTES

1. The K-Ar dating method has long been recognized to have the potential of dating young volcanic rocks (*2*), down to a few thousand years [P.-Y. Gillot and Y. Cornette, *Chem. Geol.* **59**, 205 (1986); W. Hildreth and M. Lanphere, *Geol. Soc. America Bull.* **106**, 1413 (1994)]. However, the possibility of contamination by older materials [G. B. Dalrymple, in *Means of Correlation of Quaternary Successions*, R. B. Morrison and H. E. Wright, Jr., Eds. (Univ. of Utah Press, Salt Lake City, 1967), pp. 175–194; G. H. Curtis in *Potassium Argon Dating*, O. A. Schaeffer and J. Zähringer, Eds. (Springer-Verlag, New York, 1966), pp. 151–162], or of nonatmospheric initial $^{40}Ar/^{36}Ar$ ratios, requires the use of single-crystal dating and the isochron technique to identify and overcome these problems. The ^{40}Ar-^{39}Ar dating method [C. M. Merrihue and G. Turner, *J. Geophys. Res.* **71**, 2852 (1966)], enhanced by the laser-heated single-crystal technique [D. York *et al.*, *Geophys. Res. Lett.* **8**, 1136 (1981)], has recently been extended into latest Quaternary time [(*3*); P. v. d. Bogaard, *Earth Planet. Sci. Lett.* **133**, 163 (1995)].
2. J. F. Evernden and G. H. Curtis, *Curr. Anthropol.* **6**, 343 (1965); G. B. Dalrymple, *Earth Planet. Sci. Lett.* **3**, 289 (1967).
3. Q. Hu, P. E. Smith, N. M. Evensen, D. York, *Earth Planet. Sci. Lett.* **123**, 331 (1994).
4. We use the terminology of G. B. Dalrymple and M. A. Lanphere [*Potassium-Argon Dating* (Freeman, San Francisco, 1969)] for excess argon, that is, that present from nonatmospheric sources at the time of argon closure; and inherited argon, that produced by in situ radioactive decay before the event being dated.
5. K. R. Lajoie, thesis, University of California, Berkeley (1968); in *Quaternary Stratotypes of North America*, vol. 1 (revised edition), P. F. Karrow, Ed., (Publ. 8, Quaternary Sciences Institute, Waterloo, Ontario, 1993), pp. 64–69.
6. Complete stratigraphic sections of the WCF occur at two localities: in the narrow gorge along lower Wilson Creek on the northwest shore of Mono Lake, and in the wave-cut cliffs on the southeast shore of the lake. The most distinctive feature of the WCF is the occurrence of 19 ash layers, which provide stratigraphic control throughout Mono Basin and correlation with sediments in nearby basins. Eighteen of the ash layers are rhyolitic and were erupted, as indicated by chemical data, from the Mono Craters (*5*). Crooked Meadow, underlain mostly by the Bishop Tuff, lies about 15 km east of the Mono Craters, and shows a 3.3-m-thick sequence of peat layers interbedded with 21 rhyolitic ash layers, ranging from 7 to 170 mm in thickness.
7. In the Wilson Creek section, 16 conventional ^{14}C dates on stromatolitic tufa plates and nodules, ostracod tests and marl range from about 13 to 35 ka, with two minor chronostratigraphic inversions [(*5*); L. V. Benson *et al.*, *Paleogeogr., Paleoclimatol., Paleoecol.* **78**, 241 (1990)]. Carbon-14 dates on carbonates are commonly spurious, owing mainly to possible reservoir effects and alteration. However, paleomagnetic and tephrochronological correlation of the WCF with the lacustrine Sehoo Formation of the Lahontan Basin [J. R. Liddicoat, K. R. Lajoie, A. M. Sarna-Wojcicki, *Eos* **63**, 920 (1982); K. R. Lajoie *et al.*, *Geol. Soc. Am. Abstr. Progr.* **15**, 300 (1983); A. M. Sarna-Wojcicki *et al.*, in *The Quaternary of the Unglaciated United States*, R. B. Morrison, Ed. (*Decade of North American Geology*, vol. K2, Geological Society of America, Boulder, CO, 1991), p. 117], which is dated by two ^{14}C dates on organic muck and wood [J. O. Davis, *Nev. Surv. Archeol. Res. Pap.* 7, 1 (1978)], indicates that these effects are minimal for carbonates deposited during deeper and fresher phases of Mono Lake. We tentatively conclude, therefore, that the carbonate ^{14}C dates from the WCF are accurate. To correct the ^{14}C dates from the WCF for possible changes in the concentration of atmospheric ^{14}C, we used recent dating of fossil marine coral from Barbados by accelerator mass spectrometry (AMS) ^{14}C and thermal ionization mass spectrometry (TIMS) ^{234}U-^{230}Th [E. Bard, M. Arnold, R. G. Fairbanks, B. Hamelin, *Radiocarbon* **35**, 191 (1993)]. Linear regression of 46 pairs of AMS ^{14}C and TIMS ^{234}U-^{230}Th dates yields a regression equation (age = 1.217 $\times$ ^{14}C age - 513). Further regression of the position in the Wilson Creek section versus age then yields the age estimates of 30.8 $\pm$ 0.9 ka for ash layer WCA-8, and 25.0 $\pm$ 1.0 ka for WCA-15. Fifteen conventional ^{14}C dates on peat samples from 13 horizons date the Crooked Meadow section at 11.1 to 1.1 ka (Lajoie, unpublished data). Age estimates of ash layers are obtained by simple interpolation between dated horizons, calibrated using the tree ring record [M. Stuiver and B. Becker, *Radiocarbon* **35**, 1 (1993); B. Kromer and B. Becker, *ibid.*, p. 125]. Therefore, for ash layer CMA-13, the estimated time of its eruption (deposition) is 4.6 $\pm$ 0.1 ka.
8. Ash layers WCA-8 and WCA-15 are from the south shore section of the WCF, downwind from Mono Craters, which has thicker and coarser ash layers than the dated type section at Wilson Creek. Hand-picking of 1- to 2-mm sanidine crystals, in which we avoided crystals of nonvolcanic origin, yielded mostly clear crystals, with varying amounts of adhering glass, which was removed by carefully breaking it loose. All crystals, together with flux monitors of Fish Canyon Tuff sanidine (assumed age = 27.84 million years ago), were irradiated in Cd-shielded capsules for 30 min (1 MWh) in position 5C of the McMaster Nuclear Reactor, Hamilton, Ontario, and analyzed for Ar isotope ratios in the University of Toronto Geochronology Laboratory (*3*). Isochron calculations are based on the algorithm of D. York [*Earth Planet. Sci. Lett.* **5**, 320 (1969)]. All uncertainties are given at 1σ.
9. On a diagram of $^{36}Ar/^{40}Ar$ versus $^{39}Ar/^{40}Ar$, straight lines of negative slope define systems of fixed age (given by the $^{39}Ar/^{40}Ar$ intercept), variably mixed with contaminant argon of fixed composition (given by the $^{36}Ar/^{40}Ar$ intercept = 1/295.5 for modern atmosphere).
10. Our method explores all possible subdivisions of the sphenochron into smaller wedges, for each sub-wedge, computing the MSWD of the corresponding isochron constrained to pass through modern atmosphere (*11*). It then chooses that subdivision with the smallest number of sub-wedges for which the MSWD of each sub-wedge is less than 1 and the total MSWD is a minimum.
11. The mean square weighted deviate, or MSWD, is *S*, the sum of the squares of the weighted deviations from the best fit isochron, divided by the degrees of freedom, *n*-2, where *n* is the number of data points. Its expected value is 1.
12. P. E. Damon, A. W. Laughlin, J. K. Percious, in *Radioactive Dating and Methods of Low-Level Counting* (International Atomic Energy Agency, Vienna, 1967), pp. 463–481.
13. According to recent studies on the nearby Bishop Tuff [A. N. Halliday *et al.*, *Earth Planet. Sci. Lett.* **94**, 274 (1990); (*14*)], that magma chamber could have been in existence for more than 1 million years.
14. P. v. d. Bogaard and C. Schirnick, *Geology* **23**, 759 (1995).
15. Using the diffusion constants measured by P. Zeitler [*Chem. Geol.* **65**, 167 (1987)] for sanidine from the Fish Canyon Tuff, and an estimated magma temperature of 750°C, we calculate that a 1-mm crystal would lose 90% of its argon in 8.5 days, or 99.99% in 41 days. A 25°C change in temperature would change these times by about a factor of two. About 12 hours in a 750°C magma would cause enough argon loss to change the apparent age of a 760 ka Bishop Tuff sanidine to 500 ka.
16. P. v. d. Bogaard, C. M. Hall, H.-U. Schmincke, D. York, *Nature* **342**, 523 (1989).
17. The sphenochron appears only where the range of xenocryst ages is large compared with the sample age. The absolute spread in ages represented by the sphenochrons shown here would virtually disappear into the analytical error in analyzing a sample of a million years or more in age. Sphenochrons are therefore more likely to appear in the dating of young material.

18. We thank R. C. Walter for discussions and suggestions and M. Lanphere, A. M. Sarna-Wojcicki and two anonymous reviewers for constructive comments. Supported by the University of Toronto Connaught Fund and the Natural Sciences and Engineering Research Council of Canada. Y.C. was supported by a National Research Council of Canada Postdoctoral Fellowship.

22 July 1996; accepted 3 October 1996